Counting the Isomers and Estimation of Anisotropy of Polarizability of the Selected C60 and C70 Bisadducts Promising for Organic Solar Cells

ARTICLE *in* THE JOURNAL OF PHYSICAL CHEMISTRY A · SEPTEMBER 2015

Impact Factor: 2.69 · DOI: 10.1021/acs.jpca.5b07334

3 AUTHORS, INCLUDING:

Denis Sabirov

Russian Academy of Sciences

53 PUBLICATIONS **327** CITATIONS

SEE PROFILE

R. G. Bulgakov

Ufa Scientific Center of the Russian Academy …

159 PUBLICATIONS **483** CITATIONS

SEE PROFILE

THE JOURNAL OF PHYSICAL CHEMISTRY A

Article

pubs.acs.org/JPCA

Counting the Isomers and Estimation of Anisotropy of Polarizability of the Selected C_{60} and C_{70} Bisadducts Promising for Organic Solar Cells

Denis Sh. Sabirov,* Anton O. Terentyev, and Ramil G. Bulgakov

Institute of Petrochemistry and Catalysis, Russian Academy of Sciences, 450075 Ufa, Russia

Supporting Information

ABSTRACT: Currently, bisadducts of C_{60} and C_{70} fullerenes are widely studied as electron-acceptor materials for organic solar cells. These compounds are usually used as mixtures of the positional isomers. However, as recently shown, the separate use of the purified isomers with lowest anisotropies of polarizability may enhance solar cell output parameters. To predict the structures of the compounds appropriate for this purpose, we calculated anisotropies of polarizability of four classes of fullerene bisadducts, namely, bis-[60]PCBM, [60]OQMF, bis-[70]PCBM, and [70]OQMF (18, 16, 41, and 42 positional isomers, respectively). As found, the anisotropies quadratically correlate with the interaddend distances in fullerene bisadducts, whereas there are no obvious correlations between the structures and lowest unoccupied molecular orbital levels, traditionally used for assessing the efficiency of candidates for organic solar cell electron acceptors. According to our calculations, bisadducts bis-[60]PCBM-*ee*-1, [60]OQMF-*cis*-3.2, [60]OQMF-*trans*-4.2, $cc_{1.1}cc_{2'.1}$-bis-[70]PCBM, and $cc_1cc_{2'.1}$-[70]OQMF have the lowest anisotropies of polarizability. These compounds have a primary interest for synthesis, purification, and further separate testing in solar cells. The structures of these adducts have a common feature, which we describe with the "not so close and not so far" rule: the distances between the addends in the most isotropic fullerene bisaddicts should be medium among the possible values. These are *ee*, *ef*, *cis*-3, and *trans*-4 positions in the case of the C_{60} bisadducts and *cc* bonds placed on the different poles and the same hemisphere of the C_{70} skeleton.

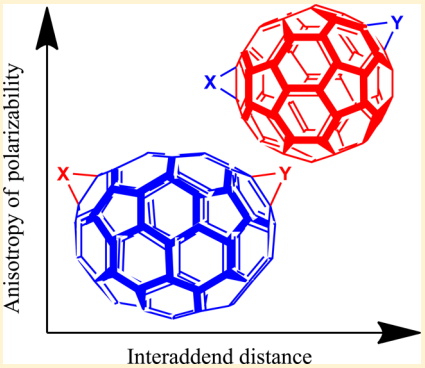

1. INTRODUCTION

Fullerene derivatives are undoubtedly promising electron-acceptor materials for organic solar cells.[1−4] Their efficiency originates from the rich π-electron systems of C_{60}/C_{70} (this facilitates the formation of the long-lived charged states) and the nature of the functionalizing moieties (this allows tuning highest occupied molecular orbital−lowest unoccupied molecular orbital (LUMO) levels, propensity for aggregation, miscibility with donor polymers, etc.).[3,4] Such C_{60} adducts as [60]PCBM, *o*-quinodimethanofullerenes (or dihydronaphthofullerenes), and their derivatives allow achieving ca. 6% power conversion efficiencies of bulk heterojunction organic solar cells (OSC).[5]

To enhance the OSC key output parameters, wide-range researches are conducted in many ways. Replacement of the usually invovled monoderivatives by the respective bis- and

Scheme 1. Structural Formulas of C_{60} and C_{70} Bisadducts under Study

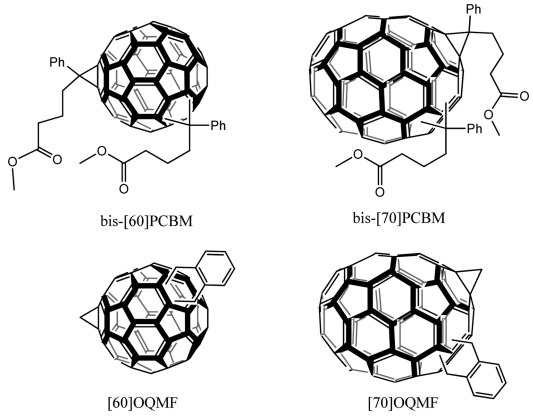

Scheme 2. Designation of the Addition of the Second Addend in the $C_{60}X_2$ Bisadducts

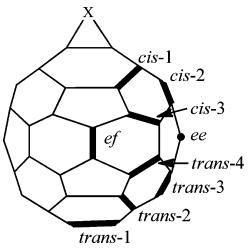

Received: July 29, 2015
Revised: August 31, 2015

DOI: 10.1021/acs.jpca.5b07334
J. Phys. Chem. A XXXX, XXX, XXX−XXX

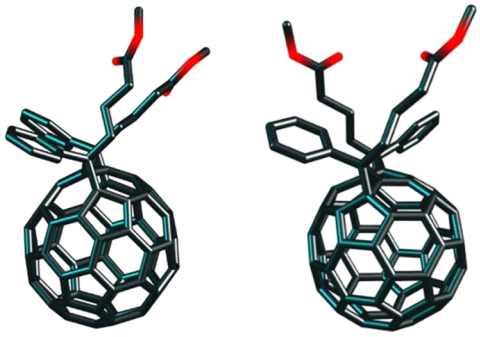

Figure 1. Isomers of bis-[60]PCBM-*cis*-2 with different spatial location of benzene rings. Hereinafter, hydrogen atoms are omitted for clarity.

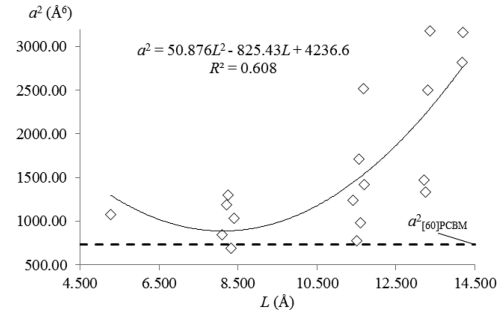

Figure 2. Dependence of anisotropy a^2 on the distance between the addends (L) in bis-[60]PCBM molecules. Line corresponds to the anisotropy of the monoadduct [60]PCBM calculated with the same method.

higher adducts of C_{60}/C_{70} becomes a common practice for this purpose.[5−15] As is known, higher fullerene adducts have several positional isomers:[16] for example, there are eight possible regioisomers in the case of $C_{60}X_2$ with symmetrical addend X (e.g., X = O or CH_2). As their chromatographic separation is difficult, bis- and higher adducts of fullerenes are mostly used as isomer mixtures.[12,13] Therefore, separating and using in OSCs the purified C_{60} bisadducts, performed in Umeyama and Imahori works,[10,11,15,17] became a fresh breeze in this field. The referenced works demonstrated that positional isomerism of the bisadducts essentially influences on the OSC efficiency. The latter may be enhanced by the use of the certain isomers instead of the mixture.

In previous work,[18] we collated our quantum chemical calculations with experimental data taken from ref 10 and found that bis-*o*-quinodimethanofullerenes (or bis(dihydronaphtho)-fullerenes) with low anisotropy of polarizability show the highest power conversion efficiencies and open-circuit voltages. This correlation seems extendable to the related fullerene derivatives tested as electron-acceptor materials (see, e.g., works[11,15,17] citing theoretical paper[18]). The role of polarizability of fullerene adducts (and its anisotropy) was discussed in our recent review,[19] which considers relations between polarizability and such influential properties of electron-acceptor materials as dielectric permittivity, wetting, and propensity for generation of the excited states (see also key original works[13,20,21]).

Relations between the structure and anisotropy of polarizability (hereinafter anisotropy) have been studied only for limited classes of fullerene derivatives (higher adducts: bis- and trisepoxides,[22] halogenides,[23,24] biscyclopropa-, bisaziridino-, bispyrrolidino-, and bis-*o*-quinodimethanofullerenes;[18,25] monoadducts: [60]PCBM,[19,26] [70]PCBM,[27] and their isomers[19,28]). At the same time, bis-PCBM and *o*-quinodimethanofullerenes with mixed functionalization become widely used in OSCs. However, the anisotropies of the mentioned compounds have not been studied. Meanwhile, the use of their least anisotropic isomers may enhance output parameters of OSCs.

In the present work, we performed the density functional theory (DFT) calculations of all possible isomers of the selected C_{60} and C_{70} bisadducts and discussed correlations between their structures and anisotropies of polarizability.

2. CALCULATION DETAILS

The PBE/3ζ DFT method (Priroda program[29,30]) was chosen for the study because it is successfully used for theoretical studies of thermodynamics and kinetics of fullerene reactions,[31−38] for IR and NMR spectra,[24,39−41] and especially for the measured mean polarizabilities of fullerenes and their derivatives (see review[19] and original works[18,22,24,33,34,37,39,42,43]).

Table 1. Elements of the Diagonalized Polarizability Tensors (α_{xx}, α_{yy}, α_{zz}), Mean Polarizabilities (α), Anisotropies of Polarizability (a^2), Relative Energies, and Interaddend Distances of the Bis-[60]PCBM Isomers

isomer	L (Å)	ΔE (kJ mol^{-1})	α_{xx} (Å^3)	α_{yy} (Å^3)	α_{zz} (Å^3)	α (Å^3)	a^2 (Å^6)
cis-2.1	8.089	10.40	116.76	131.65	150.22	132.88	842.82
cis-2.2	8.249	14.77	114.75	127.83	155.50	132.69	1299.04
cis-3.1	5.283	11.97	111.04	138.28	147.39	132.24	1073.43
cis-3.2	8.218	9.15	110.00	139.26	147.95	132.40	1186.14
cis-3.3	11.417	3.13	109.57	142.96	146.41	132.98	1241.88
ee-1	8.315	0.42	116.05	137.63	145.33	133.00	691.32
ee-2	11.514	0.24	115.09	139.95	145.35	133.47	781.25
trans-1.1	13.360	3.57	112.13	120.16	172.09	134.79	3178.17
trans-1.2	14.188	3.39	112.72	119.59	172.05	134.79	3158.84
trans-2.1	11.678	2.15	111.02	126.00	167.01	134.68	2520.06
trans-2.2	13.298	2.25	111.52	125.58	167.05	134.72	2500.40
trans-2.3	14.182	2.03	110.79	124.34	169.38	134.84	2821.82
trans-3.1	11.556	0.24	116.90	124.94	161.74	134.53	1714.60
trans-3.2	11.695	0.12	116.07	128.68	158.45	134.40	1420.39
trans-3.3	13.255	0.00	115.12	130.94	156.92	134.32	1336.43
trans-4.1	8.392	4.05	113.10	137.73	149.56	133.46	1038.09
trans-4.2	11.600	3.85	114.64	135.52	150.74	133.63	985.65
trans-4.3	13.211	3.99	114.44	129.52	158.09	134.02	1475.09

DOI: 10.1021/acs.jpca.5b07334
J. Phys. Chem. A XXXX, XXX, XXX−XXX

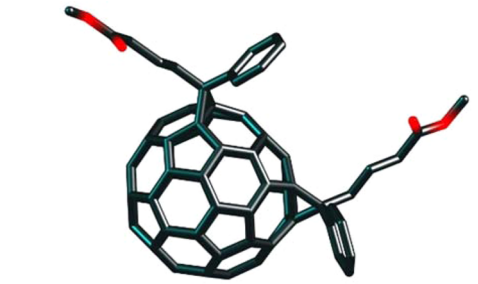

bis-[60]PCBM-*ee*-1

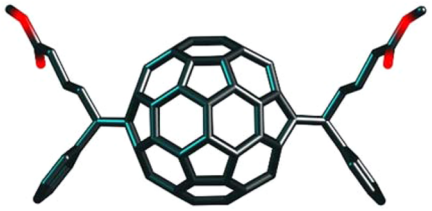

bis-[60]PCBM-*trans*-1.1

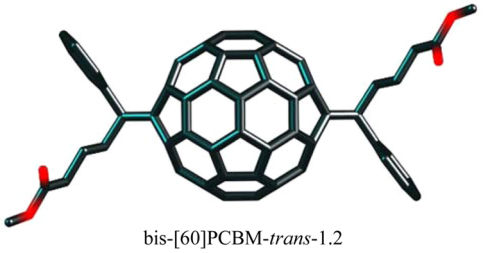

bis-[60]PCBM-*trans*-1.2

Figure 3. Bis-[60]PCBM-*ee*-1 and two bis-[60]PCBM-*trans*-1, isomers with the lowest and highest anisotropies, respectively.

After standard DFT optimizations and vibration modes solving (to prove that all the stationary points, respective to the molecules under study, are minima of the potential energy surfaces), the components of polarizability tensors $\boldsymbol{\alpha}$ were calculated in terms of the finite field approach as the second-order derivatives of the total energy E with respect to the homogeneous external electric field **F**:

$$\alpha_{ij} = -\frac{\partial^2 E}{\partial F_i \partial F_j} \quad (1)$$

Tensors $\boldsymbol{\alpha}$ were calculated in the arbitrary coordinate system and then diagonalized. Their eigenvalues α_{ii} (i = x, y, and z) allow calculating the mean polarizability α and its anisotropy a^2:

$$\alpha = \frac{1}{3}(\alpha_{xx} + \alpha_{yy} + \alpha_{zz}) \quad (2)$$

$$a^2 = \frac{1}{2}((\alpha_{yy} - \alpha_{xx})^2 + (\alpha_{zz} - \alpha_{yy})^2 + (\alpha_{zz} - \alpha_{xx})^2) \quad (3)$$

We studied the following bisadducts of C_{60} and C_{70}: bis-[60]PCBM, bis-[70]PCBM, *o*-quinodimethane-methano[60]-fullerenes ([60]OQMF) (Scheme 1), and *o*-quinodimethane-methano[70]fullerenes ([70]OQMF). The optimized structures of the studied compounds are available as Supporting Information.

3. RESULTS AND DISCUSSION

3.1. Bis-[60]PCBM Isomers. [60]PCBM is a well-known electron acceptor, traditionally used as a reference compound in experimental OSC studies.[5] Its mean polarizability and anisotropy have been previously calculated by DFT methods.[19,26] The [60]PCBM structure contains a cyclopropane moiety >C(Ph)$(CH_2)_3COOCH_3$ with two different substituents. [60]PCBM has eight unequivalent double bonds, to which the attachment of another addend is possible (Scheme 2).

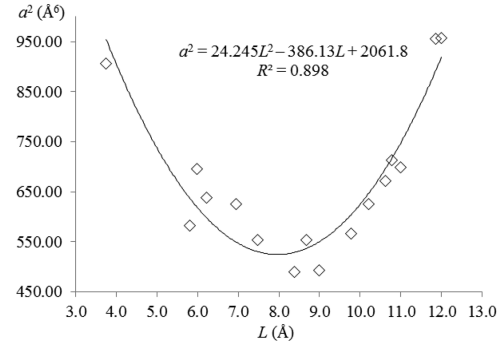

Figure 4. Dependence of anisotropy a^2 on the distance between the addends (L) in the [60]OQMF molecules.

Counting the theoretically achievable structures of bis-[60]PCBM, we took into account the dissymmetry of addends that leads to appearance of their different spatial locations. If two functionalized double bonds are symmetrically placed on the fullerene cage (*cis*-2, *e*, and *trans*-1 positions), we find two isomers of bis-[60]PCBM having the same addition pattern but differing in the relative arrangement of the substituents in the attached moieties. For example, two isomers correspond to *cis*-2 addends position. These have the Ph rings placed in the same (bis-[60]PCBM-*cis*-2.1) or in different (bis-[60]PCBM-*cis*-2.2) directions about the imaginary surface involving carbon atoms of the cyclopropane cycles (Figure 1). We numerate such positional isomers with Arabic numbers giving 1 to the isomer with the closest Ph arrangement and 2 with the remotest one. In other positions (*cis*-3, *trans*-2, *trans*-3, and *trans*-4), three different spatial arrangements of Ph are possible due to the unsymmetrical location of the functionalized bonds on the fullerene cage. These isomers similarly obtain Arabic indices from 1 to 3, which correspond to the increasing distance between the Ph rings. Note that we failed with optimization of bis-[60]PCBM-*cis*-1. Obviously, this structure does not exist due to the steric hindrances arising when two bulky addends >C(Ph)$(CH_2)_3COOCH_3$ should be neighboring on the fullerene cage.

The considerations above indicate 18 possible bis-[60]PCBM isomers. Their energetic, structural, and polarizability characteristics are shown in Table 1. In this set, bis-[60]PCBM-*trans*-3.3 has the lowest total energy. Nonetheless, the calculated relative energies ΔE manifest thermodynamic equiprobability of their formation (ΔE values are less than 15 kJ mol^{-1}). To describe the diversity of the obtained structures, we used the distance L between the centers of the Ph rings as an auxiliary geometric parameter. We should here mention one structural feature of the bis-[60]PCBM set. The distances L are not smoothly varied from *cis*-2 to *trans*-1 positions, and their clustering near the certain values is observed: these are ∼8 Å (for *cis*-2.1, *cis*-2.2, *cis*-3.2, *e*-1, and *trans*-4.1), ∼11 Å (for *cis*-3.3, *e*-2, *trans*-2.1, *trans*-3.1, *trans*-3.2, and *trans*-4.2), ∼13 Å (for *trans*-1.1, *trans*-2.2, *trans*-3.3, and *trans*-4.3), and ∼14 Å (for *trans*-1.2 and *trans*-2.3 isomers).

Bis-[60]PCBM isomers are characterized with different anisotropies a^2. The a^2 versus L plot shows that anisotropy

DOI: 10.1021/acs.jpca.5b07334
J. Phys. Chem. A XXXX, XXX, XXX−XXX

Table 2. Elements of the Diagonalized Polarizability Tensors (α_{xx}, α_{yy}, α_{zz}), Mean Polarizabilities (α), Anisotropies of Polarizability (a^2), Relative Energies, and Interaddend Distances of the [60]OQMF Isomers

isomer	L (Å)	ΔE (kJ mol^{-1})	α_{xx} (Å^3)	α_{yy} (Å^3)	α_{zz} (Å^3)	α (Å^3)	a^2 (Å^6)
cis-1.1	3.751	4.94	89.49	92.35	120.91	100.92	905.59
cis-1.2	5.817	0.00	91.13	93.92	116.54	100.53	582.73
cis-2.1	5.991	21.27	89.05	95.71	118.12	100.96	695.80
cis-2.2	6.951	20.77	89.32	96.72	117.19	101.08	625.24
cis-3.1	6.224	20.46	90.39	94.81	117.58	100.92	638.78
cis-3.2	8.388	20.19	91.35	96.27	115.52	101.05	489.60
ee-1	7.470	6.78	91.77	94.66	116.60	101.01	553.24
ee-2	9.767	6.66	91.77	94.75	116.92	101.15	566.74
ef-1	8.685	8.71	89.15	98.28	115.89	101.11	554.20
trans-1.1	12.000	11.39	89.49	92.21	121.69	101.13	956.50
trans-2.1	11.002	9.70	91.48	93.56	118.89	101.31	698.67
trans-2.2	11.862	9.53	89.51	92.64	121.87	101.34	955.73
trans-3.1	10.206	7.02	89.71	96.80	117.49	101.33	625.14
trans-3.2	10.785	6.97	89.41	95.89	118.76	101.36	713.35
trans-4.1	8.984	11.64	91.23	96.20	115.51	100.98	493.48
trans-4.2	10.627	11.72	90.56	94.45	118.21	101.07	672.11

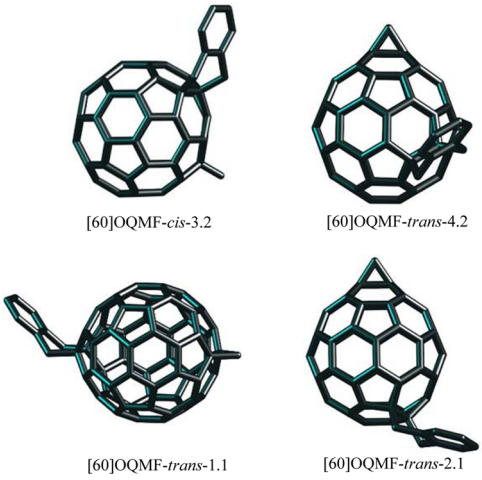

Figure 5. Regioisomers of [60]OQMF with the lowest (*cis*-3.2 and *trans*-4.2) and highest (*trans*-1.1 and *trans*-2.1) anisotropies.

correlates with the distance between the centers of the benzene rings (Figure 2). The correlation may be satisfactorily described with a quadratic polynomial (similar to the previously studied case of the nonsubstituted [2 + 1]-cycloadducts of C_{60}[18,19]); its minimum corresponds to two equatorial isomers. Among them, bis-[60]PCBM-*ee*-1 (Figure 3) has the lowest values of anisotropy, so it is expected to be the most appropriate electron-acceptor for OSC application. Its antipodes bis-[60]PCBM-*trans*-1.1 and bis-[60]PCBM-*trans*-1.2 demonstrate highest a^2 values (Figure 3). Additionally, comparison between a^2 values of the monoadduct [60]PCBM (736.08 Å^6; PBE/3ζ[19]) and bis-[60]PCBM isomers shows that the aforementioned bis-[60]PCBM-*ee*-1 isomer is the only bisadduct with lower anisotropy than its precursor [60]PCBM.

Scheme 3. Designations of Addend Positions in the C_{70} Fullerene[a]

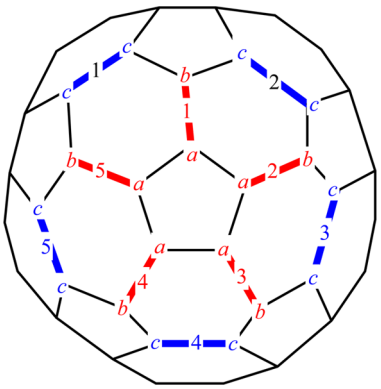

[a]One of the polar pentagons is in the center of the illustration.

3.2. [60]OQMF Isomers. *o*-Quinodimethane-methano[60]-fullerenes ([60]OQMF) are another class of the C_{60} derivatives promising for OSCs. At the moment, these compounds have been experimentally tested only as a mixture of the isomers.[14] Their molecules contain two types of functionalizing moieties (cyclopropane and dihydronaphthalene). Therefore, we meet slightly different situations in this case as compared to bis-[60]PCBM. First, positions *ef* and *ee* (*e*-face and *e*-edge) in [60]OQMF become unequivalent due to different nature of the

Table 3. Elements of the Diagonalized Polarizability Tensors (α_{xx}, α_{yy}, α_{zz}), Mean Polarizabilities (α), and Anisotropies of Polarizability (a^2) of the Monoadducts [70]PCBM[a]

	PBE/3ζ					B3LYP/6-311G(d,p)	
isomer	α_{xx}	α_{yy}	α_{zz}	α	a^2	α	a^2
ab-[70]PCBM	113.29	118.43	155.46	129.06	1588.09	116.9	1193.17
$cc_{1,1}$-[70]PCBM	124.15	111.73	147.58	127.82	994.10	114.1	671.84
$cc_{1,2}$-[70]PCBM	122.38	111.51	150.17	128.02	1192.45	114.5	952.11

[a]A Comparison between the PBE/3ζ and B3LYP/6-311G(d,p) calculations (taken from the previous work[27]). Values of α and a^2 are in Å^3 and Å^6, respectively.

DOI: 10.1021/acs.jpca.5b07334
J. Phys. Chem. A XXXX, XXX, XXX−XXX

Table 4. Elements of the Diagonalized Polarizability Tensors (α_{xx}, α_{yy}, α_{zz}), Mean Polarizabilities (α), Anisotropies of Polarizability (a^2), Relative Energies, and Interaddend Distances of the Bis-[70]PCBM Isomers

isomer	L (Å)	ΔE (kJ mol^{-1})	α_{xx} (Å^3)	α_{yy} (Å^3)	α_{zz} (Å^3)	α (Å^3)	a^2 (Å^6)
$ab_{1,1}ab_{1',1}$	12.518	0.42	142.03	130.93	194.94	155.97	3510.08
$ab_{1,1}ab_{1',2}$	13.470	0.00	143.27	134.16	189.74	155.72	2666.31
$ab_{1,1}ab_{2',2}$	13.493	0.41	132.38	137.61	198.85	156.28	4097.12
$ab_{1,1}ab_{2',1}$	12.575	0.07	132.62	142.88	192.24	155.91	3048.63
$ab_{1,1}ab_{3',2}$	14.959	3.25	128.35	137.08	203.95	156.46	5131.09
$ab_{1,1}ab_{3',1}$	13.629	2.97	130.60	138.31	199.85	156.26	4321.44
$ab_{1,1}ab_{3,1}$	5.809	27.65	134.89	138.52	187.45	153.62	2585.58
$ab_{1,1}ab_{3,2}$	8.145	16.73	143.43	136.44	182.68	154.18	1863.62
$ab_{1,2}ab_{3',2}$	15.027	3.10	137.32	128.92	202.83	156.36	4912.35
$ab_{1,2}ab_{3,1}$	8.051	17.72	150.19	136.52	176.56	154.42	1243.08
$ab_{1,1}cc_{2',2}$	12.390	13.48	152.76	127.12	183.44	154.44	2385.12
$ab_{1,1}cc_{2',1}$	8.686	11.53	157.06	128.01	176.54	153.87	1788.80
$ab_{1,1}cc_{3',2}$	13.457	13.35	130.22	142.79	192.16	155.06	3215.41
$ab_{1,1}cc_{3',1}$	10.940	11.36	129.81	149.13	184.90	154.61	2343.86
$ab_{1,1}cc_{4',2}$	14.957	11.50	139.02	128.23	199.34	155.53	4406.10
$ab_{1,1}cc_{4',1}$	13.630	9.86	140.75	130.55	194.43	155.24	3532.61
$ab_{1,1}cc_{3,2}$	8.196	20.32	131.81	152.26	175.78	153.29	1452.27
$ab_{1,1}cc_{3,1}$	5.575	20.32	130.92	146.63	181.22	152.93	1986.79
$ab_{1,1}cc_{4,2}$	11.539	11.28	159.32	129.53	172.39	153.75	1447.93
$ab_{1,1}cc_{4,1}$	8.356	13.74	153.41	130.40	176.79	153.53	1614.17
$ab_{1,2}cc_{2',2}$	13.407	13.44	153.01	129.71	180.14	154.28	1911.44
$ab_{1,2}cc_{2',1}$	10.795	11.99	158.72	130.02	172.36	153.70	1401.17
$ab_{1,2}cc_{3',2}$	14.914	13.42	132.34	138.92	194.16	155.14	3457.45
$ab_{1,2}cc_{3',1}$	13.502	11.13	132.29	144.67	187.20	154.72	2488.48
$ab_{1,2}cc_{3,2}$	11.356	19.46	133.26	158.40	169.52	153.73	1035.57
$ab_{1,2}cc_{3,1}$	8.196	21.49	132.86	151.44	175.86	153.39	1395.23
$cc_{1,1}cc_{1',1}$	4.484	28.51	168.64	123.82	160.75	151.07	1717.40
$cc_{1,1}cc_{1',2}$	8.594	24.32	167.46	124.46	163.85	151.92	1707.05
$cc_{1,1}cc_{2',1}$	9.201	19.73	136.40	158.34	162.32	152.35	584.27
$cc_{1,1}cc_{2',2}$	10.734	21.95	137.02	151.07	170.82	152.97	864.77
$cc_{1,1}cc_{3',1}$	13.835	21.86	186.85	131.95	142.61	153.80	2541.88
$cc_{1,1}cc_{3',2}$	13.580	23.73	142.34	127.90	192.11	154.12	3403.97
$cc_{1,1}cc_{2,1}$	8.046	32.41	145.23	136.74	172.89	151.62	1072.23
$cc_{1,1}cc_{2,2}$	8.244	38.60	143.75	132.95	178.17	151.62	1672.70
$cc_{1,1}cc_{3,1}$	13.169	22.20	173.86	128.24	157.73	153.27	1605.35
$cc_{1,1}cc_{3,2}$	11.609	23.84	168.19	129.12	161.95	153.09	1321.18
$cc_{1,2}cc_{1',2}$	12.257	27.61	161.68	125.88	170.22	152.59	1659.87
$cc_{1,2}cc_{2',2}$	13.301	23.80	137.57	143.55	179.47	153.53	1540.81
$cc_{1,2}cc_{3',2}$	14.894	25.35	141.18	125.35	196.66	154.40	4206.12
$cc_{1,2}cc_{2,2}$	5.588	46.06	141.93	135.75	177.17	151.62	1497.94
$cc_{1,2}cc_{3,2}$	8.419	25.84	164.75	126.74	167.90	153.13	1573.88

addends. Second, the cyclopropane moiety is small enough to be a neighbor of the dihydronaphthalene fragment. Hence, *cis*-1 isomers of [60]OQMF are able to exist in contrast to bis-[60]PCBM-*cis*-1. Third, both of the addends are symmetric, so the number of variations is smaller than in the previous case (for *ef* and *trans*-1 positions, there are only one isomer; otherwise, there are two isomers for each position). The considerations above lead to 16 positional isomers of [60]OQMF. To distinguish them, we use a distance L between the central atom of the cyclopropane moiety and the center of the benzene ring of another addend. The second indices for isomer counting are attributed according to the L values as in the bis-[60]PCBM case (increasing with L). Anisotropy is quadratically correlated with interaddend distance L (Figure 4). The calculated polarizability properties of [60]OQMF are listed in Table 2. The lowest anisotropies are typical for *cis*-3.2 and *trans*-4.2 isomers as the highest one for *trans*-1.1 and *trans*-2.1, shown in Figure 5.

3.3. Bis-[70]PCBM Isomers. Previously, monoadducts [70]PCBM have been synthesized.[44] Their structures have >C(Ph)$(CH_2)_3$COOCH$_3$ addends attached to *ab* and *cc* bonds (bond designations are according to ref 45). Previously, polarizabilities and hyperpolarizabilities of these adducts have been theoretically studied[27,28]. Therefore, we briefly compared our calculation with the previous one and found them consistent. Indeed, both methods show almost equal mean polarizabilities of the isomers and the increase in the anisotropy in the series: $cc_{1,1}$-[70]PCBM < $cc_{1,2}$-[70]PCBM < *ab*-[70]PCBM (Table 3).

The mixtures of isomeric bis-[70]PCBM are also used in OSC,[5] so we chose these compounds as one of the objectives for our study. We proposed that the functionalization of the C_{70} cage is possible only via the most reactive *ab* and *cc* bonds. As in the case of the C_{60} derivatives, we used the distance L between the Ph rings in the bisadduct molecules for numerically

DOI: 10.1021/acs.jpca.5b07334
J. Phys. Chem. A XXXX, XXX, XXX−XXX

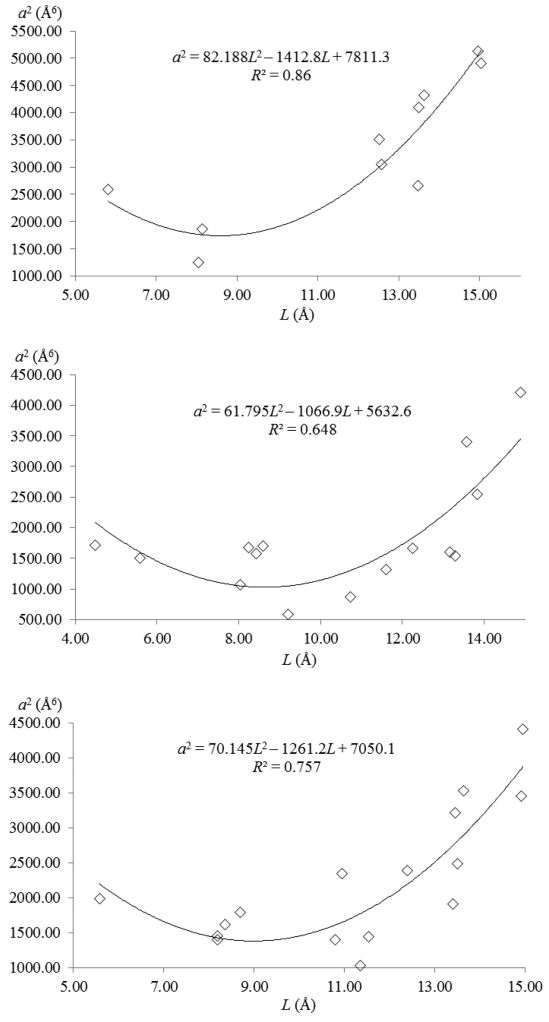

Figure 6. Dependence of anisotropy a^2 on the distance between the addends (L) in bis-[70]PCBM with *ab* (a), *cc* (b), and mixed *ab-cc* functionalization (c).

describing their structural diversity. We designate isomeric bis-[70]PCBM structures by numbering the bonds to which the addends are attached. These are five *ab* and five *cc* bonds numbered from 1 to 5 on the first pole of the C_{70} molecule and from 1′ to 5′ on the other (Scheme 3). Additional Arabic indices reflect, as above, the dissimilar orientation of the substituents in the cyclopropane rings of the isomers.

These considerations uncover 31 isomeric structures of bis-[70]PCBM. These include 10 isomers with the functionalized *ab* bonds, 15 isomers with the functionalized *cc* bonds, and 16 isomers with "mixed" *ab-cc* functionalization. Note that there are no bis-[70]PCBM isomers with the closest location of addends (ab_1ab_2 isomers, in which the nearest *ab* bonds would have been functionalized). The calculated energetic, structural, and polarizability characteristics of bis-[70]PCBM are shown in Table 4. As there are three groups of bis-[70]PCBM isomers, we separately scrutinized their a^2 versus L plots (Figure 6). Quadratic correlations between a^2 and L were found in each group. The most anisotropic isomers in the mentioned groups are $ab_{1.1}ab_{3'.2}$, $ab_{1.1}cc_{4'.2}$, and $cc_{1.2}cc_{3'.2}$. Anisotropy decreases in the series of the most isotropic isomers of the mentioned subgroups of bis-[70]PCBM $ab_{1.2}ab_{3.1} > ab_{1.2}cc_{3.2} > cc_{1.1}cc_{2'.1} \approx cc_{1.1}cc_{2'.2}$ (Figures 7−9). Among all bis-[70]PCBM regioisomers, $cc_1cc_{2'.1}$-bis-[70]PCBM has the lowest a^2 value.

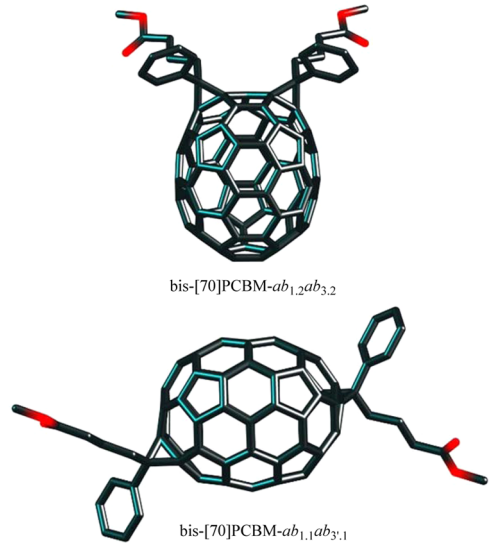

Figure 7. Molecules of $ab_{1.2}ab_{3.2}$ and $ab_{1.1}ab_{3'.1}$ isomers of bis-[70]PCBM with the lowest and highest anisotropies in the *ab* set.

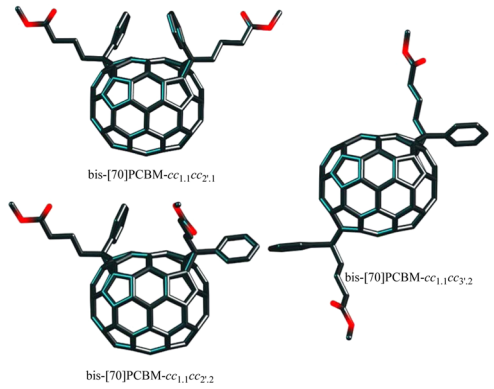

Figure 8. Molecules of $cc_{1.1}cc_{2'.1}$, $cc_{1.1}cc_{2'.2}$, and $cc_{1.1}cc_{3'.2}$ isomers of bis-[70]PCBM. The two first species have the lowest anisotropies; the last has the highest one.

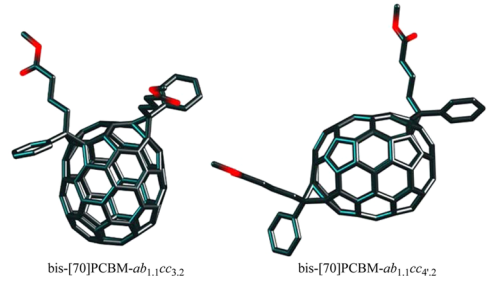

Figure 9. Isomers $ab_{1.1}cc_{3.2}$ and $ab_{1.1}cc_{4'.2}$ of bis-[70]PCBM with the lowest and highest anisotropies of the *ab-cc* set.

3.4. [70]OQMF Isomers. To counting [70]OQMF, we applied the algorithm, similar to the bis-[70]PCBM case with bond numbering shown in Scheme 3. The first bond designation in the [70]OQMF bisadducts corresponds to the site of $>CH_2$ addition; the second designation describes the position of the *o*-quinodimethane moiety (type and number of bond) and its orientation (1 or 2) due to the nonplanarity. This allows elucidating 42 isomers, for which the calculated properties are collected in Table 5. Analyzing the a^2 versus L plots, we found that some [70]OQMF isomers have lower

DOI: 10.1021/acs.jpca.5b07334
J. Phys. Chem. A XXXX, XXX, XXX−XXX

Table 5. Elements of the Diagonalized Polarizability Tensors (α_{xx}, α_{yy}, α_{zz}), Mean Polarizabilities (α), Anisotropies of Polarizability (a^2), Relative Energies, and Interaddend Distances of the [70]OQMF Isomers

isomer	L (Å)	ΔE (kJ mol^{-1})	α_{xx} (Å^3)	α_{yy} (Å^3)	α_{zz} (Å^3)	α (Å^3)	a^2 (Å^6)
$ab_1ab_{1'.1}$	11.520	5.08	113.58	105.32	145.72	121.54	1366.49
$ab_1ab_{1'.2}$	11.521	5.12	113.59	105.31	145.73	121.54	1367.82
$ab_1ab_{2.1}$	3.760	4.20	105.43	110.52	148.39	121.45	1653.05
$ab_1ab_{2'.1}$	11.650	5.61	112.84	106.18	145.82	121.61	1351.71
$ab_1ab_{2.2}$	5.829	0.00	107.09	112.22	143.54	120.95	1167.57
$ab_1ab_{2'.2}$	12.472	5.71	106.08	111.00	147.88	121.65	1565.50
$ab_1ab_{3.1}$	6.991	23.34	114.56	105.18	145.06	121.60	1304.36
$ab_1ab_{3'.1}$	12.679	8.72	106.72	110.66	147.52	121.63	1519.55
$ab_1ab_{3.2}$	6.033	23.45	112.85	105.71	145.94	121.50	1382.06
$ab_1ab_{3'.2}$	13.161	8.86	110.97	105.01	149.02	121.66	1709.86
$ab_1cc_{2.1}$	5.826	9.63	134.08	105.99	117.86	119.31	596.67
$ab_1cc_{2'.1}$	8.817	20.94	132.80	106.25	120.70	119.92	530.15
$ab_1cc_{2.2}$	3.760	14.36	108.80	106.22	145.87	120.29	1476.36
$ab_1cc_{2'.2}$	11.177	20.85	111.58	106.17	144.14	120.63	1265.91
$ab_1cc_{3.1}$	8.395	30.72	107.35	133.26	119.98	120.20	503.39
$ab_1cc_{3'.1}$	10.879	20.37	107.22	134.96	118.15	120.11	585.71
$ab_1cc_{3.2}$	6.265	30.91	106.88	110.58	144.57	120.68	1294.50
$ab_1cc_{3'.2}$	12.379	20.38	107.19	108.63	146.43	120.75	1485.63
$ab_1cc_{4.1}$	9.775	21.02	133.21	105.92	120.93	120.02	560.78
$ab_1cc_{4'.1}$	11.980	17.87	138.08	106.29	116.52	120.30	789.78
$ab_1cc_{4.2}$	7.525	21.20	112.16	106.02	143.28	120.48	1197.02
$ab_1cc_{4'.2}$	13.070	17.98	107.91	106.39	148.43	120.91	1705.66
$cc_1ab_{1.1}$	5.823	4.21	107.64	110.02	143.03	120.23	1173.73
$cc_1ab_{1'.1}$	9.654	16.59	104.27	115.85	142.02	120.71	1121.98
$cc_1ab_{1.2}$	3.756	8.66	104.12	111.03	147.03	120.73	1593.06
$cc_1ab_{1'.2}$	10.634	16.72	105.90	113.53	142.88	120.77	1144.05
$cc_1ab_{2.1}$	8.413	27.87	114.61	106.44	142.27	121.11	1057.67
$cc_1ab_{2'.1}$	11.037	16.22	108.41	111.11	143.17	120.90	1121.59
$cc_1ab_{2.2}$	6.259	28.02	110.47	108.08	144.49	121.01	1244.68
$cc_1ab_{2'.2}$	12.402	16.24	110.31	106.27	146.29	120.96	1456.60
$cc_1ab_{3.1}$	8.724	18.52	115.79	104.40	142.06	120.75	1119.15
$cc_1ab_{3'.1}$	12.619	14.86	105.08	146.63	111.43	121.04	1502.46
$cc_1cc_{1'.1}$	6.220	32.52	105.23	133.83	117.88	118.98	616.16
$cc_1cc_{1'.2}$	9.089	33.29	105.33	113.32	140.63	119.76	1028.32
$cc_1cc_{2.1}$	6.926	43.23	132.91	108.64	115.19	118.91	473.10
$cc_1cc_{2'.1}$	8.899	28.35	131.83	108.41	117.66	119.30	417.33
$cc_1cc_{2.2}$	6.006	43.67	106.76	109.15	142.38	119.43	1189.61
$cc_1cc_{2'.2}$	10.549	28.42	111.48	106.41	141.92	119.94	1106.75
$cc_1cc_{3.1}$	10.606	31.29	106.08	133.62	118.07	119.26	571.69
$cc_1cc_{3'.1}$	12.011	29.95	106.42	137.32	114.28	119.34	773.77
$cc_1cc_{3.2}$	9.019	31.48	105.43	113.22	140.58	119.74	1021.92
$cc_1cc_{3'.2}$	12.539	29.89	105.86	108.48	145.42	119.92	1468.49

anisotropies than the others and, hence, fall from the main trend (Figure 10).

These isomers have *o*-quinodimethane added to *cc* bond and are turned toward the equatorial belt of the C_{70} skeleton. In this subset (and among all possible [70]OQMF isomers), $cc_1cc_{2'.1}$-[70]OQMF is characterized with the lowest a^2 value. Its counterparts with highest anisotropies $ab_1ab_{3'.2}$ and $ab_1cc_{4'.2}$ have addends in the remotest positions (Figure 11; the interaddend distances are ca. 13 Å).

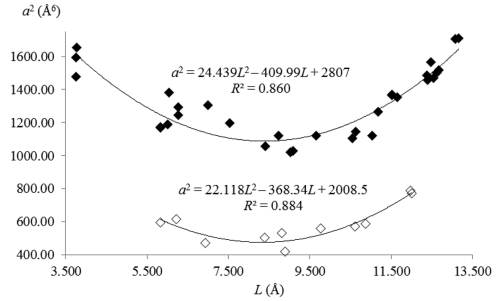

Figure 10. Dependence of anisotropy a^2 on the distance between the addends (L) in [70]OQMF.

4. CONCLUSION

In the present paper, we have calculated anisotropies of polarizability of four classes of fullerene bisadducts promising for OSC to predict which isomers should be more isotropic and presumably more efficient for this application. The numbers of possible bis-[60]PCBM, [60]OQMF, bis-[70]PCBM, and [70]OQMF isomers are 18, 16, 31, and 42, respectively. Their mean polarizabilities lie in the narrow intervals (132.24–134.84, 100.53–101.36, 151.62–156.46, and 118.98–121.66 Å^3

DOI: 10.1021/acs.jpca.5b07334
J. Phys. Chem. A XXXX, XXX, XXX−XXX

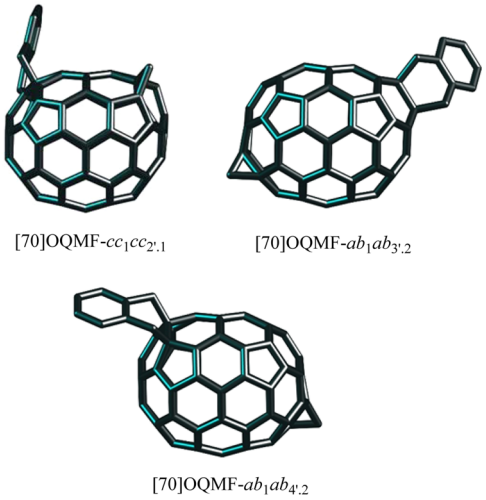

Figure 11. [70]OQMF-$cc_1cc_{2',1}$ with the lowest anisotropy of polarizability and two isomers ($ab_1ab_{3',2}$ and with $ab_1cc_{4',2}$) with the highest one.

for bis-[60]PCBM, [60]OQMF, bis-[70]PCBM, and [70]OQMF). Total energies of the isomers within the selected groups do not differ significantly. Hence, anisotropy of polarizability is the most sensitive property that reflects even minimal structural dissimilarity of the studied compounds. All the obtained correlations between anisotropies and interaddend distances are described with quadratic polynomials with satisfactory accuracy (R^2 = 0.608−0.898).

As known, open-circuit voltages can be predicted with the LUMO energies of fullerene adducts.[46,47] We think that the use of LUMO levels for choosing an appropriate fullerene adduct within the isomeric series is problematic as there are no obvious correlations between the LUMO energies and structures within the regioisomeric sets (see Figures S1−S4 in Supporting Information). In contrast, anisotropies of isomeric fullerene bisadducts are correlated with their structure.

On the basis of the DFT calculations and previously found correlation between the anisotropy and key OSC output parameters,[18] the following most isotropic fullerene derivatives are recommended for separate testing in bulk-heterojunction OSCs to enhance their efficiency: bis-[60]PCBM-*ee*-1, [60]-OQMF-*cis*-3.2, [60]OQMF-*trans*-4.2, $cc_{1,1}cc_{2',1}$-bis-[70]PCBM, and $cc_1cc_{2',1}$-[70]OQMF. The structures of these bisadducts have a common feature, which consists in the balanced location of addends, so we can formulate the following "not so close and not so far" rule: the distances between the addends in the most isotropic fullerene bisaddicts should be medium from the possible values. In the case of the C_{60} fullerene bisadducts, it means that addends should be located in equatorial (*ee* or *ef*) or pre-equatorial (*cis*-3 or *trans*-4) positions. Applied to the C_{70} bisadducts, this rule means that functionalizing moieties should be attached to *cc* bonds located on the different poles and the same hemisphere of the C_{70} skeleton.

In conclusion, we also note that synthetic methodologies to highly selective syntheses of C_{60} and C_{70} bisadducts are intensively developed. As stressed in a recent report,[48] the use of endometallofullerenes or tethered moieties added to the fullerene cage allows tuning the addition pattern and, hence, increasing the regioselectivity (see also original works[17,49−53]). We hope that our rule may be used by experimentalists without need of quantum chemical calculations and facilitate their hard task of finding appropriate fullerene-based electron acceptors for organic solar cells.

■ ASSOCIATED CONTENT

Supporting Information

The Supporting Information is available free of charge on the ACS Publications website at DOI: 10.1021/acs.jpca.5b07334.

LUMO versus interaddend distance plots for the studied compounds. (PDF)

Cartesian coordinates of the optimized fullerene bisadducts. (ZIP)

■ AUTHOR INFORMATION

Corresponding Author

*E-mail: diozno@mail.ru.

Notes

The authors declare no competing financial interest.

■ REFERENCES

(1) Hoppe, H.; Sariciftci, N. S. Organic Solar Cells: An Overview. *J. Mater. Res.* **2004**, *19*, 1924−1945.

(2) Blom, P. W. M.; Mihailetchi, V. D.; Koster, L. J. A.; Markov, D. E. Device Physics of Polymer:Fullerene Bulk Heterojunction Solar Cells. *Adv. Mater.* **2007**, *19*, 1551−1566.

(3) Liu, T.; Troisi, A. What Makes Fullerene Acceptors Special as Electron Acceptors in Organic Solar Cells and How to Replace Them. *Adv. Mater.* **2013**, *25*, 1038−1041.

(4) Troshin, P. A.; Hoppe, H.; Renz, J.; Egginger, M.; Mayorova, J. Y.; Goryachev, A. E.; Peregudov, A. S.; Lyubovskaya, R. N.; Gobsch, G.; Sariciftci, N. S.; et al. Material Solubility-Photovoltaic Performance Relationship in the Design of Novel Fullerene Derivatives for Bulk Heterojunction Solar Cells. *Adv. Funct. Mater.* **2009**, *19*, 779−788.

(5) Li, C.-Z.; Yip, H.-L.; Jen, A. K.-Y. Functional Fullerenes for Organic Photovoltaics. *J. Mater. Chem.* **2012**, *22*, 4161−4177.

(6) Lenes, M.; Wetzelaer, G.-J. A. H.; Kooistra, F. B.; Veenstra, S. C.; Hummelen, J. C.; Blom, P. W. M. Fullerene Bisadducts for Enhanced Open-Circuit Voltages and Efficiencies in Polymer Solar Cells. *Adv. Mater.* **2008**, *20*, 2116−2119.

(7) Lenes, M.; Shelton, S. W.; Sieval, A. B.; Kronholm, D. F.; Hummelen, J. C.; Blom, P. W. M. Electron Trapping in Higher Adduct Fullerene-Based Solar Cells. *Adv. Funct. Mater.* **2009**, *19*, 3002−3007.

(8) Dyer-Smith, C.; Reynolds, L. X.; Bruno, A.; Bradley, D. D. C.; Haque, S. A.; Nelson, J. Triplet Formation in Fullerene Multi-Adduct Blends for Organic Solar Cells and Its Influence on Device Performance. *Adv. Funct. Mater.* **2010**, *20*, 2701−2708.

(9) Meng, X.; Zhang, W.; Tan, Z.; Li, Y.; Ma, Y.; Wang, T.; Jiang, L.; Shu, C.; Wang, C. Highly Efficient and Thermally Stable Polymer Solar Cells with Dihydronaphthyl-Based [70]Fullerene Bisadduct Derivative as the Acceptor. *Adv. Funct. Mater.* **2012**, *22*, 2187−2193.

(10) Kitaura, S.; Kurotobi, K.; Sato, M.; Takano, Y.; Umeyama, T.; Imahori, H. Effects of Dihydronaphthyl-Based [60]fullerene Bisadduct Regioisomers on Polymer Solar Cell Performance. *Chem. Commun.* **2012**, *48*, 8550−8552.

(11) Umeyama, T.; Imahori, H. Design and Control of Organic Semiconductors and Their Nanostructures for Polymer−Fullerene-Based Photovoltaic Devices. *J. Mater. Chem. A* **2014**, *2*, 11545−11560.

(12) Meng, X.; Zhao, G.; Xu, Q.; Tan, Z.; Zhang, Z.; Jiang, L.; Shu, C.; Wang, C.; Li, Y. Effects of Fullerene Bisadduct Regioisomers on Photovoltaic Performance. *Adv. Funct. Mater.* **2014**, *24*, 158−163.

(13) Kim, K.-H.; Kang, H.; Kim, H. J.; Kim, P. S.; Yoon, S. C.; Kim, B. J. Effects of Solubilizing Group Modification in Fullerene Bis-Adducts on Normal and Inverted Type Polymer Solar Cells. *Chem. Mater.* **2012**, *24*, 2373−2381.

(14) He, D.; Du, X.; Xiao, Z.; Ding, L. Methanofullerenes, $C_{60}(CH_2)_n$ (n = 1, 2, 3), as Building Blocks for High-Performance Acceptors Used in Organic Solar Cells. *Org. Lett.* **2014**, *16*, 612−615.

(15) Tao, R.; Umeyama, T.; Kurotobi, K.; Imahori, H. Effects of Alkyl Chain Length and Substituent Pattern of Fullerene Bis-Adducts on

DOI: 10.1021/acs.jpca.5b07334
J. Phys. Chem. A XXXX, XXX, XXX−XXX

Film Structures and Photovoltaic Properties of Bulk Heterojunction Solar Cells. *ACS Appl. Mater. Interfaces* **2014**, *6*, 17313−17322.
(16) Thilgen, C.; Diederich, F. Structural Aspects of Fullerene ChemistryA Journey through Fullerene Chirality. *Chem. Rev.* **2006**, *106*, 5049−5135.
(17) Tao, R.; Umeyama, T.; Higashino, T.; Koganezawa, T.; Imahori, H. A Single Cis-2 Regioisomer of Ethylene-Tethered Indene Dimer−fullerene Adduct as an Electron-Acceptor in Polymer Solar Cells. *Chem. Commun.* **2015**, *51*, 8233−8236.
(18) Sabirov, D. S. Anisotropy of Polarizability of Fullerene Higher Adducts for Assessing the Efficiency of Their Use in Organic Solar Cells. *J. Phys. Chem. C* **2013**, *117*, 9148−9153.
(19) Sabirov, D. S. Polarizability as a Landmark Property for Fullerene Chemistry and Materials Science. *RSC Adv.* **2014**, *4*, 44996−45028.
(20) Koster, L. J. A.; Shaheen, S. E.; Hummelen, J. C. Pathways to a New Efficiency Regime for Organic Solar Cells. *Adv. Energy Mater.* **2012**, *2*, 1246−1253.
(21) Bernardo, B.; Cheyns, D.; Verreet, B.; Schaller, R. D.; Rand, B. P.; Giebink, N. C. Delocalization and Dielectric Screening of Charge Transfer States in Organic Photovoltaic Cells. *Nat. Commun.* **2014**, *5*, 3245.
(22) Sabirov, D. S.; Bulgakov, R. G. Polarizability of Oxygen-Containing Fullerene Derivatives $C_{60}O_n$ and $C_{70}O$ with Epoxide/oxidoannulene Moieties. *Chem. Phys. Lett.* **2011**, *506*, 52−56.
(23) Tang, S.-W.; Feng, J.-D.; Qiu, Y.-Q.; Sun, H.; Wang, F.-D.; Chang, Y.-F.; Wang, R.-S. Electronic Structures and Nonlinear Optical Properties of Highly Deformed Halofullerenes C_{3v} $C_{60}F_{18}$ and D_{3d} $C_{60}Cl_{30}$. *J. Comput. Chem.* **2010**, *31*, 2650−2657.
(24) Sabirov, D. S.; Garipova, R. R.; Bulgakov, R. G. General Formula for Accurate Calculation of Halofullerenes Polarizability. *Chem. Phys. Lett.* **2012**, *523*, 92−97.
(25) Sabirov, D. S.; Tukhbatullina, A. A.; Bulgakov, R. G. Dependence of Static Polarizabilities of $C_{60}X_n$ Fullerene Cycloadducts on the Number of Added Groups X = CH_2 and NH (n = 1−30). *Comput. Theor. Chem.* **2012**, *993*, 113−117.
(26) Zhang, C. DFT Study on Methanofullerene Derivative [6,6]-Phenyl-C_{61} Butyric Acid Methyl Ester. *Acta Phys.-Chim. Sin.* **2008**, *24*, 1353−1358.
(27) Akhtari, K.; Hassanzadeh, K.; Fakhraei, B.; Hassanzadeh, H.; Akhtari, G.; Zarei, S. A. First Hyperpolarizability Orientation in [70]PCBM Isomers: A DFT Study. *Comput. Theor. Chem.* **2014**, *1038*, 1−5.
(28) Zhang, C.-R.; Han, L.-H.; Zhe, J.-W.; Jin, N.-Z.; Shen, Y.-L.; Yuan, L.-H.; Wu, Y.-Z.; Liu, Z.-J. Electronic Structures and Optical Properties of Phenyl C_{71} Butyric Acid Methyl Esters. *J. Nanomater.* **2013**, *2013*, e612153.
(29) Perdew, J. P.; Burke, K.; Ernzerhof, M. Generalized Gradient Approximation Made Simple. *Phys. Rev. Lett.* **1996**, *77*, 3865−3868.
(30) Laikov, D. N.; Ustynyuk, Y. A. PRIRODA-04: A Quantum-Chemical Program Suite. New Possibilities in the Study of Molecular Systems with the Application of Parallel Computing. *Russ. Chem. Bull.* **2005**, *54*, 820−826.
(31) Shestakov, A. F. Reactivity of Fullerene C_{60}. *Russ. J. Gen. Chem.* **2008**, *78* (4), 811−821.
(32) Sabirov, D. S.; Khursan, S. L.; Bulgakov, R. G. Quantum Chemical Modeling of Ozone Addition to C_{60} Fullerene. *Fullerenes, Nanotubes, Carbon Nanostruct.* **2008**, *16*, 534−537.
(33) Sabirov, D. S.; Bulgakov, R. G.; Khursan, S. L.; Dzhemilev, U. M. A New Approach to the Estimation of the Fullerene Reactivity in 1,3-Dipolar Addition Based on Polarizability Indices. *Dokl. Phys. Chem.* **2009**, *425*, 54−56.
(34) Sabirov, D. S.; Bulgakov, R. G. Reactivity of Fullerene Derivatives $C_{60}O$ and $C_{60}F_{18}$ (C_{3v}) in Terms of Local Curvature and Polarizability. *Fullerenes, Nanotubes, Carbon Nanostruct.* **2010**, *18*, 455−457.
(35) Tuktarov, A. R.; Akhmetov, A. R.; Sabirov, D. S.; Khalilov, L. M.; Ibragimov, A. G.; Dzhemilev, U. M. Catalytic [2 + 1] Cycloaddition of Diazo Compounds to [60]Fullerene. *Russ. Chem. Bull.* **2009**, *58*, 1724−1730.
(36) Tuktarov, A. R.; Korolev, V. V.; Sabirov, D. S.; Dzhemilev, U. M. Catalytic Cycloaddition of Diazoalkanes to Fullerene C_{60}. *Russ. J. Org. Chem.* **2011**, *47* (1), 41−47.
(37) Sabirov, D. S.; Garipova, R. R.; Bulgakov, R. G. Density Functional Theory Study on the Decay of Fullerenyl Radicals $RC_{60}^{\bullet}$, $ROC_{60}^{\bullet}$, and $ROOC_{60}^{\bullet}$ (R = Tert-Butyl and Cumyl) and Polarizability of the Formed Fullerene Dimers. *J. Phys. Chem. A* **2013**, *117*, 13176−13183.
(38) Sabirov, D. S.; Garipova, R. R.; Bulgakov, R. G. What Fullerene is More Reactive Towards Peroxyl Radicals? A Comparative DFT Study on $ROO^{\bullet}$ Addition to C_{60} and C_{70} Fullerenes. *Fullerenes, Nanotubes, Carbon Nanostruct.* DOI:**2015**23105110.1080/1536383X.2015.1060963.
(39) Bulgakov, R. G.; Galimov, D. I.; Sabirov, D. S. New Property of the Fullerenes: The Anomalously Effective Quenching of Electronically Excited States Owing to Energy Transfer to the C_{70} and C_{60} Molecules. *JETP Lett.* **2007**, *85*, 632−635.
(40) Pankratyev, E. Y.; Tulyabaev, A. R.; Khalilov, L. M. How Reliable Are GIAO Calculations of ^{1}H and ^{13}C NMR Chemical Shifts? A Statistical Analysis and Empirical Corrections at DFT (PBE/3z) Level. *J. Comput. Chem.* **2011**, *32*, 1993−1997.
(41) Tulyabaev, A. R.; Khalilov, L. M. ^{13}C NMR in Fullerene Chemistry: Structure/Shift Relationsip and Quantum-Chemical Predictions. In *Fullerenes, Chemistry, Natural Sources, and Technological Applications;* Nova Publishers: New York, 2014; pp 95−122.
(42) Sabirov, D. S.; Garipova, R. R.; Bulgakov, R. G. Polarizability of C_{70} Fullerene Derivatives $C_{70}X_8$ and $C_{70}X_{10}$. *Fullerenes, Nanotubes, Carbon Nanostruct.* **2012**, *20*, 386−390.
(43) Sabirov, D. S. From Endohedral Complexes to Endohedral Fullerene Covalent Derivatives: A Density Functional Theory Prognosis of Chemical Transformation of Water Endofullerene $H_2O@C_{60}$ upon Its Compression. *J. Phys. Chem. C* **2013**, *117*, 1178−1182.
(44) Wienk, M. M.; Kroon, J. M.; Verhees, W. J. H.; Knol, J.; Hummelen, J. C.; van Hal, P. A.; Janssen, R. A. J. Efficient Methano[70]fullerene/MDMO-PPV Bulk Heterojunction Photovoltaic Cells. *Angew. Chem.* **2003**, *115*, 3493−3497.
(45) Tumanskii, B. L. An ESR Study of Radical Reactions of C_{60} and C_{70}. *Russ. Chem. Bull.* **1996**, *45*, 2267−2278.
(46) Frost, J. M.; Faist, M. A.; Nelson, J. Energetic Disorder in Higher Fullerene Adducts: A Quantum Chemical and Voltammetric Study. *Adv. Mater.* **2010**, *22*, 4881−4884.
(47) Morvillo, P.; Bobeico, E. Tuning the LUMO Level of the Acceptor to Increase the Open-Circuit Voltage of Polymer-Fullerene Solar Cells: A Quantum Chemical Study. *Sol. Energy Mater. Sol. Cells* **2008**, *92*, 1192−1198.
(48) Echegoyen, L.; Cerón, M.; Izquierdo, M. International Conference "Advanced Carbon Nanostructures", June 29−July 03, 2015, St. Petersburg, Russia, p 3.
(49) Sergeyev, S.; Schär, M.; Seiler, P.; Lukoyanova, O.; Echegoyen, L.; Diederich, F. Synthesis of *Trans*-1, *Trans*-2, *Trans*-3, and *Trans*-4 Bisadducts of C_{60} by Regio- and Stereoselective Tether-Directed Remote Functionalization. *Chem. - Eur. J.* **2005**, *11*, 2284−2294.
(50) Cardona, C. M.; Kitaygorodskiy, A.; Ortiz, A.; Herranz, M. A.; Echegoyen, L. The First Fulleropyrrolidine Derivative of $Sc_3N@C_{80}$: Pronounced Chemical Shift Differences of the Geminal Protons on the Pyrrolidine Ring. *J. Org. Chem.* **2005**, *70*, 5092−5097.
(51) Cardona, C. M.; Kitaygorodskiy, A.; Echegoyen, L. Trimetallic Nitride Endohedral Metallofullerenes: Reactivity Dictated by the Encapsulated Metal Cluster. *J. Am. Chem. Soc.* **2005**, *127*, 10448−10453.
(52) Tao, R.; Umeyama, T.; Higashino, T.; Koganezawa, T.; Imahori, H. Synthesis and Isolation of *Cis*-2 Regiospecific Ethylene-Tethered Indene Dimer−[70]Fullerene Adduct for Polymer Solar Cell Applications. *ACS Appl. Mater. Interfaces*, **2015**71667610.1021/acsami.5b04351.
(53) Cerón, M. R.; Izquierdo, M.; Pi, Y.; Atehortúa, S. L.; Echegoyen, L. Tether-Directed Bisfunctionalization Reactions of C_{60} and C_{70}. *Chem. - Eur. J.* **2015**, *21*, 7881−7885.

DOI: 10.1021/acs.jpca.5b07334
J. Phys. Chem. A XXXX, XXX, XXX−XXX